Electrostatic Contributions to the Binding of Ca^{2+} in Calbindin D_{9k}†

Sara Linse,*,‡ Charlotta Johansson,‡ Peter Brodin,§ Thomas Grundström,§ Torbjörn Drakenberg,‡ and Sture Forsén‡

Physical Chemistry 2, Chemical Centre, Lund University, P.O. Box 124, S-221 00 Lund, Sweden, and Unit of Applied Cell and Molecular Biology, University of Umeå, S-901 87 Umeå, Sweden

Received July 5, 1990; Revised Manuscript Received August 17, 1990

ABSTRACT: A set of accurate experimental data is provided for Ca^{2+} ion binding to calbindin D_{9k}, a protein in the calmodulin superfamily of intracellular regulatory proteins. The study comprises both the role of protein surface charges and the effects of added electrolyte. The two macroscopic Ca^{2+}-binding constants K_1 and K_2 are determined for the wild-type and eight mutant calbindins in 0, 0.05, 0.10, and 0.15 M KCl from titrations in the presence of Quin 2 or 5,5′-Br_2BAPTA. The mutations involve replacement of surface carboxylates (of Glu17, Asp19, Glu26, and Glu60) with the corresponding amides. It is found that K_1K_2 may decrease by a factor of up to 2.5×10^5 (triple mutant in 0.15 M KCl as compared to the wild-type protein in 0 M KCl). Ca^{2+}-binding constants of the individual Ca^{2+} sites (microscopic binding constants) have also been determined. The positive cooperativity of Ca^{2+} binding, previously observed at low salt concentration [Linse et al. (1987) *Biochemistry 26*, 6723–6735], is also present at physiological ionic strength and amounts to 5 kJ·mol^{-1} at 0.15 M KCl. The electrolyte concentration and some of the mutations are found to affect the cooperativity. ^{39}K NMR studies show that K^+ binds weakly to calbindin. Two-dimensional ^1H NMR studies show, however, that potassium binding does not change the protein conformation, and the large effect of KCl on the Ca^{2+} affinity is thus of unspecific nature. Two-dimensional ^1H NMR has also been used to assess the structural consequences of the mutations through assignments of the backbone NH and $C_\alpha H$ resonances of six mutants. Comparison with the corresponding chemical shifts in the wild-type protein shows that the mutations E17Q, E26Q, and E60Q do not affect the structure of the protein. The D19N mutation causes a minor rearrangement in the loop region, but the three-dimensional structure appears to be largely similar to the wild type also in this mutant. Assignment of one double (E17Q+E26Q) and the triple (E17Q+D19N+E26Q) mutant shows that the chemical shift effects of the individual substitutions are essentially additive. The presented data may serve as a basis for evaluating different theoretical models of electrostatic interactions in proteins.

Despite the central role played by electrostatic interactions in proteins, there is still considerable uncertainty regarding the treatment of such interactions by theoretical methods. Rigorous statistical mechanical treatment using truly microscopic models that deal with the system at an atomic level becomes exceedingly complex and intractable even for molecules of modest size (Harvey, 1989; Honig & Gilson, 1988). Therefore, different approximations must be introduced and tested against experimental data. Presently there are, however, few detailed and systematic experimental studies displaying significant electrostatic effects. One of the most extensive sets of experimental data published to date concerns pK_a shifts of a histidine in subtilisin BPN′ due to annihilation of charges in the protein (Thomas et al., 1985; Sternberg et al., 1987). The observed pK_a shifts are, however, small (<0.5 pK_a unit); this makes tests of electrostatic models (Sternberg et al., 1987; Gilson & Honig, 1987) less decisive.

We have recently shown that the number and identity of negative surface residues have a pronounced influence on the Ca^{2+} affinity of calbindin D_{9k} (Linse et al., 1988) through effects on the Ca^{2+} on-rate (Martin et al., 1990). It has also been observed that the stability of this protein toward denaturation increases when negative surface charges are neutralized (Akke & Forsén, 1990). Protein surface charges have also been shown to influence a number of other protein functions, for example, the transport properties of the Ca^{2+}-activated K^+ channel (MacKinnon et al., 1989), the interaction between calmodulin and some of its target enzymes (Weber et al., 1989), and the binding of cytochrome c_2 to the *Rhodobacter sphaeroides* reaction center in optimal orientation for rapid electron transfer (Long et al., 1989).

The protein used in the present study, calbindin D_{9k}, is a small (M_r = 8500), globular, and highly stable (Wendt et al., 1988) member of the calmodulin superfamily of intracellular calcium-binding proteins (Kretsinger, 1987), in which a pair of EF-hand (Kretsinger & Nockolds, 1973) Ca^{2+}-binding sites constitutes the functional unit. Calbindin D_{9k} contains one such unit, with one of the sites differing from the archetypal EF hand, and binds two Ca^{2+} ions strongly, with association constants of 2×10^6 to 6×10^8 M^{-1} depending on the ionic strength (Bredderman & Wasserman, 1974; Bryant, 1985; Bryant & Andrews, 1984; Linse et al., 1987). The crystal structure of calcium-loaded calbindin has been determined to high resolution (Szebenyi & Moffat, 1986). A particular feature of this protein is that the spatial arrangement of charged amino acid side chains is markedly asymmetrical with an excess of negative charges where the Ca^{2+}-binding sites are situated. In addition to the four carboxylate side chains that are directly ligated to the Ca^{2+} ions, 7 of the remaining 13 carboxylate groups of calbindin occur within 12 Å of the Ca^{2+} sites (see Figure 1). Recent ^1H NMR[1] studies indicate that

† This work was supported by the Swedish Natural Science Research Council (NFR, K-KU-2545-300) and the Swedish National Board for Technical Development (STU 512/89/576 and 732/89/866). The NMR spectrometer was purchased with generous grants from the Knut and Alice Wallenberg Foundation and the Swedish Council for Planning and Coordination of Research (FRN).

* Correspondence should be addressed to this author.
‡ Lund University.
§ University of Umeå.

0006-2960/91/0430-154$02.50/0

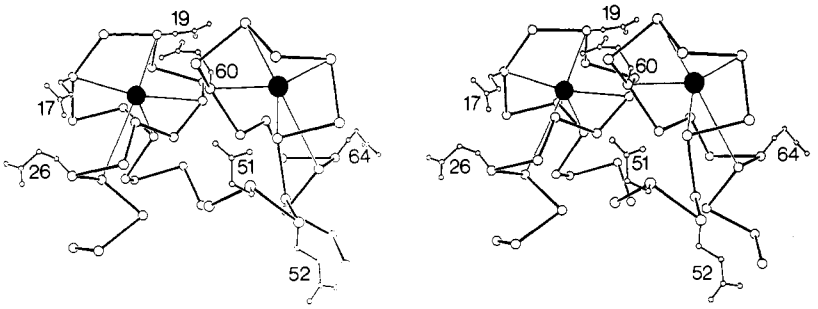

FIGURE 1: Stereoview of the Ca^{2+}-binding sites of calbindin D_{9k} based on a crystallographic analysis. Some of the negatively charged surface residues are explicitly shown. Figure kindly provided by D. Szebenyi, Cornell University.

the structure in solution is largely similar to that in the crystal both in the Ca^{2+}-loaded (Drakenberg et al., 1989; Kördel et al., 1989; Akke et al., 1990; Linse et al., 1990) and the Ca^{2+}-free (Skelton et al., 1990a,b; Linse et al., 1990) forms.

Here we present a detailed experimental study of the two macroscopic Ca^{2+}-binding constants of bovine calbindin D_{9k}. The dependence on both electrolyte concentration and surface charge is addressed in a study of the wild-type protein and eight mutants in which four surface carboxylate groups have been replaced by the corresponding amides. The measured effects on the free energy of binding two Ca^{2+} ions are in the range (1.8–30.7) ± 1.0 kJ·mol^{-1} (0.3–5.4 pK_a units), and the results are sufficiently detailed to provide a rigorous test of theoretical models for electrostatic effects in proteins. One successful model, based on a Monte Carlo approach, has recently been presented (Svensson et al., 1990a,b). We have chosen to study structural effects of the charge substitutions by comparing ^{1}H NMR assignments of backbone resonances and NOE connectivities with the same parameters in the wild-type protein. Through evaluation of double and triple mutants the additivity in chemical shift perturbations can be addressed.

Experimental Procedures

Wild-type calbindin D_{9k}, the E60Q mutant, and all possible single, double, and triple mutants involving the substitutions E17Q, D19N, and E26Q have been produced from synthetic genes (Brodin et al., 1990) and purified as previously described (Linse et al., 1987), except that the urea step was replaced by a heat denaturation step in order to avoid deamidation of the proteins (Chazin et al., 1990; Johansson et al., 1990). Quin 2 (Tsien, 1980) was from Fluka (Buchs, Switzerland) and 5,5′-Br_2BAPTA (Tsien, 1980) was from Molecular Probes (Eugene, OR). $^{113}Cd(NO_3)_2$ was prepared from cadmium metal enriched to 90% in ^{113}Cd (Oak Ridge National Laboratory, Oak Ridge, TN). All other chemicals were of the highest purity commercially available.

Ca^{2+}-Binding Constants. Each protein (20–30 μM) was titrated with Ca^{2+} in the presence of 0, 0.05, 0.10, and 0.15 M KCl and the tetrapotassium salt of either Quin 2 or 5,5′-Br_2BAPTA (30 μM) in 2 mM Tris-HCl buffer at pH 7.5 and 25 °C as described (Linse et al., 1987, 1988). Quin 2 was used for wild type, E17Q, E26Q, and E60Q. 5,5′-Br_2BAPTA was used for the remaining mutants as well as for E17Q and E26Q.

Since all information that can be extracted from experimental data resides in the data points themselves, the most direct way of obtaining this information is to perform a least-squares fit to the measured quantity, in the present case the absorbance as a function of total Ca^{2+} concentration. The absorbance changes result from Ca^{2+} binding to the chelator only but depend on how the total calcium is distributed between free Ca^{2+}, chelator-bound Ca^{2+}, and protein-bound Ca^{2+}. This distribution is governed by the Ca^{2+} affinities for the chelator (one binding constant) and protein (two macroscopic binding constants) and the concentrations of chelator and protein.

The two macroscopic binding constants of the protein K_1 and K_2 were hence obtained from least-squares fits to the absorbance at 263 nm as a function of total Ca^{2+} concentration. The analysis was based entirely on concentration. Fixed parameters in the fit were KDQ, the Ca^{2+} dissociation constant of the chelator, CQ_i, the chelator concentration at titration point i, $CATOT_i$, the total Ca^{2+} concentration at point i including initial and added Ca^{2+}, and CP_i, protein concentration (by weight of lysophilized protein) at point i. CQ_i, CP_i, and $CATOT_i$ include corrections for the dilutions imposed by Ca^{2+} additions. Variable parameters in the fit were K_1, K_2, AMAX, AMIN, and F. K_1 and K_2 are macroscopic binding constants that refer to the binding of the first and second Ca^{2+} ion to the protein irrespective of what site is occupied in the protein. AMAX and AMIN are the absorbances that the initial solution would have if it were completely Ca^{2+}-free or contained saturating amounts of Ca^{2+}, respectively. F is a correction factor that accounts for the fact that the protein concentration obtained by weight could be off by 10–20% due to residual water in lyophilized protein and because small (0.7–1.5 mg) quantities were used. For each set of variable parameters the Newton–Raphson method was used to solve the free Ca^{2+} concentration Y at each titration point i from the equation

$$Y = \mathrm{CATOT}_i - \frac{YCQ_i}{Y + \mathrm{KDQ}} - \frac{FCP_i(K_1Y + 2K_1K_2Y^2)}{1 + K_1Y + K_1K_2Y^2}$$

which states that the free Ca^{2+} equals the total Ca^{2+} subtracted by the Quin 2 bound Ca^{2+} and the protein-bound Ca^{2+}. The absorbance of Quin 2 at 263 nm decreases when Quin 2 binds Ca^{2+}, and the absorbance at point i could then be calculated as

$$\mathrm{Abs}_{\mathrm{calculated},i} = [\mathrm{AMAX} - (\mathrm{AMAX} - \mathrm{AMIN})Y/(Y + \mathrm{KDQ})]CQ_i/CQ_1$$

where CQ_1 is the initial chelator concentration. Thus the changes in absorbance were assumed to arise from the chelator only (which was experimentally verified). The error square

[1] Abbreviations: Quin 2, 2-[[2-[bis(carboxymethyl)amino]-5-methylphenoxy]methyl]-6-methoxy-8-[bis(carboxymethyl)amino]-quinoline; 5,5′-Br_2BAPTA, 5,5′-dibromo-1,2-bis(*o*-aminophenoxy)-ethane-*N*,*N*,*N*′,*N*′-tetraacetic acid; EDTA, ethylenediaminetetraacetic acid; EGTA, ethylene glycol bis(β-aminoethyl ether)-*N*,*N*,*N*′,*N*′-tetraacetic acid; NMR, nuclear magnetic resonance; COSY, *J*-correlated spectroscopy; NOE, nuclear Overhauser enhancement; NH, amide proton; C_αH, proton bound to α-carbon. The one-letter codes for amino acids are used in the mutant definitions. E17Q thus stands for a mutant protein with glutamine substituted for glutamate at position 17.

Table I: Calcium-Binding Constants, K_a, of Chelators at Different KCl Concentrations

condition	K_a (M^{-1})	
	Quin 2	5,5′-Br_2BAPTA
low salt concn	1.9×10^8	1.0×10^7
0.05 M KCl	2.5×10^7	1.3×10^6
0.10 M KCl	1.2×10^7	6.3×10^5
0.15 M KCl	8.4×10^6	4.4×10^5

sum ESS was obtained by summing over all points in the titration:

$$\mathrm{ESS} = \sum_i (\mathrm{Abs}_{\mathrm{calculated},i} - \mathrm{Abs}_{\mathrm{measured},i})^2$$

The variable parameters were iterated in a separate procedure until an optimal fit (minimum ESS) was found.

K_1 and K_2, expressed in molar concentration units, were used to calculate the free energy of binding of two Ca^{2+} ions, $\Delta G_{tot} = -RT \ln (K_1K_2)$, and a lower limit of the free energy of interaction between the sites (cf. Results and Discussion), $-\Delta\Delta G_{\eta=1} = RT \ln (4K_2/K_1)$. For each titration the uncertainties were estimated from a series of least-squares fits to the data with K_1 (or K_2) fixed at different values. The uncertainties in each parameter were taken to include all values of the parameter that, for both titrations on a specific combination of protein and KCl concentration, give less than two times the error square sum of the optimal fit. The product of K_1 and K_2 (and hence ΔG_{tot}) is well-defined in all cases, but when the cooperativity is high ($K_2 \gg K_1$), the separation into K_1 and K_2 (and hence $-\Delta\Delta G_{\eta=1}$) becomes uncertain, due to the inherent properties of cooperativity (Weber, 1975). The uncertainties do not include errors in the Ca^{2+} affinities for the chelators that were determined separately at different KCl concentrations as summarized in Table I, with the least-squares fits based entirely on concentration. As for K_1 and K_2, the concentration of K^+ ions is not entered into the calculations. The values of K, K_1, and K_2 thus contain all salt effects. The K values obtained at 0.10 M KCl agree with those reported by Tsien (1980), and the two chelators gave the same results for E17Q and E26Q at each value of KCl concentration.

^1H NMR. ^{1}H NMR spectra were obtained at 500.13 MHz on a GE OMEGA 500 spectrometer.

Assignments. For assignments, 5 mM protein samples were prepared in 450 μL of H_2O (5% D_2O) with 13 mM Ca^{2+} at pH 6.0 and 27 °C. The following types of two-dimensional ^{1}H NMR spectra were recorded: for (E17Q+D19N+E26Q), COSY, relayed COSY, HOHAHA (30-ms mixing time), and NOESY (200-ms mixing time); for E17Q, D19N, E26Q, (E17Q+E26Q), and E60Q, COSY, relayed COSY, and NOESY (200 ms). In addition, a 200-ms NOESY was recorded for (E17Q+D19N+E26Q) in 99.9% D_2O, after freeze-drying once from 99.5% D_2O (after adjustment of pH to 6.0 with 0.4% DCl) and once from 99.9% D_2O. Since most shift perturbations due to the mutations are small and many COSY cross-peaks are well separated, most of the chemical shifts were initially obtained simply by comparison with the COSY and relayed COSY spectra of the Ca-loaded wild-type calbindin D_{9k} (Kördel et al., 1989). These preliminary assignments were confirmed by following the NH–NH connectivities in the 200-ms NOESY, a procedure that also provided assignments of the cross-peaks in more crowded areas of the spectrum. This procedure resulted in assignment of all NH and C_αH shifts except for Lys1, Asp/Asn19, and the four proline residues. In addition, in the mutant (E17Q+E26Q), Gly18 and Ser44 were not assigned. A proline in position 20 and fast exchange of both G18 and D19 (N19) NH's make it difficult to assign D19 without more complete assignments.

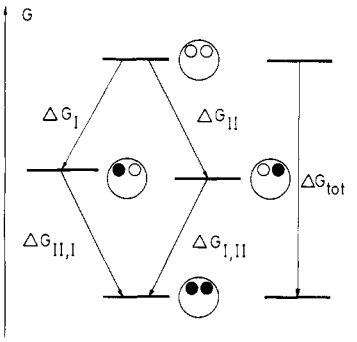

FIGURE 2: Free energy diagram of the binding of identical ligands to a two-site protein. Note that the free ligands are omitted from the figure, but of course contribute to the ΔG's.

Determination of the Relative Affinities for the Sites. During Ca^{2+} titrations one-dimensional spectra were recorded for 5 mM protein samples in 10 mM phosphate buffer at pH 7.5 in H_2O (with 5% D_2O). The starting solutions contained less than 0.1 mol of Ca^{2+}/mol of protein. The initial volume was 500 μL, and $CaCl_2$ was added in 5-μL portions of a 100 mM stock solution at pH 7.5 with a Carlsberg pipet to obtain high reproducibility in the addition volume. These titrations could not be used for determining K_1 and K_2, which are several orders of magnitude larger than the inverse protein concentration used in ^{1}H NMR. They do, however, provide additional information as to the relative affinities of the two sites, $\eta = K_{II}/K_I$ (cf. Figure 2). With 5 mM protein (with its counterions) and 10 mM phosphate buffer, we find it reasonable to assume that the values of K_1 and K_2 are close to those determined in the presence of chelator in 50 mM KCl. To obtain η from one ^{1}H NMR titration, the intensities of several well-resolved resonances were first corrected for the dilution imposed by the Ca^{2+} additions at each titration point. The corrected intensities were then plotted versus total Ca^{2+} concentration, as exemplified in Figure 3A. During the titration there will be four different protein species in solution: the apo form (with population P_0), the Ca_2 form (P_2), and two forms with one Ca^{2+} ion bound (P_I and P_{II}); cf. Figure 2. The populations P_0 and P_2 and the sum of P_I and P_{II} are given by K_1 and K_2, while the distribution between P_I and P_{II} is given by the site-binding constants K_I and K_{II}. Due to slow exchange the spectrum obtained at each titration point will be a superposition of the population-weighted spectra of the four forms. Each proton in the protein has a specific ^{1}H NMR shift, and the shift could be different in all four forms. It could also be the same in any combination of these forms, although it is not likely that a proton has the same chemical shift in both Ca_1 forms but not in the Ca_2 form. The expected behavior (intensity versus total Ca^{2+}) of resonances representing the other combinations is displayed in Figure 3B.

Since the present data do not provide information as to which site is the strongest, we will in the following use the labels A and B instead of I and II, with B representing the site with the highest Ca^{2+} affinity. Signals from protons with the same chemical shift in the Ca_2 form and one of the Ca_1 forms will increase close to linearly with increasing Ca^{2+} concentration (curves 5 and 6 in Figure 3A), whereas signals from protons with the same chemical shift in the apo form and one of the Ca_1 forms will decrease almost linearly (curves 1 and 2 in Figure 3A). The intensities of these signals at a given Ca^{2+} concentration are given by the equation

$$I_{\mathrm{calculated}} = \mathrm{IMAX}(P_0 j_0 + P_A j_A + P_B j_B + P_2 j_2)$$

where P_0, P_A, P_B, and P_2 are the populations of the four states

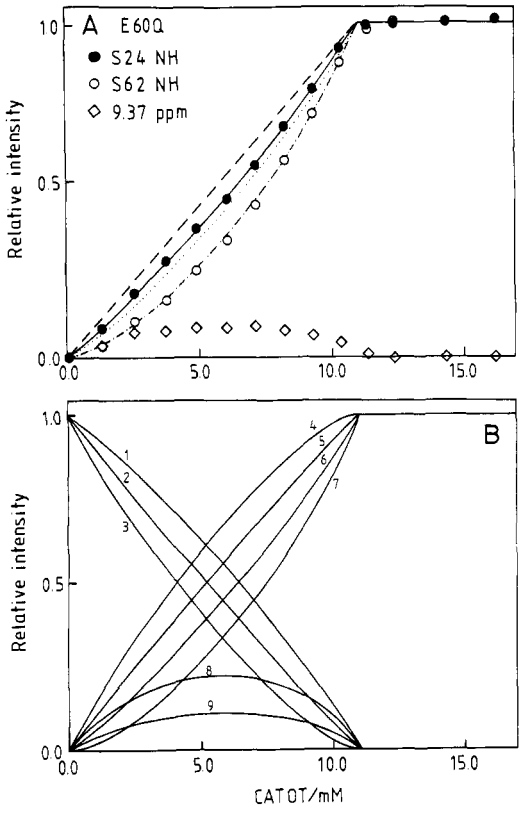

FIGURE 3: (A) Intensities of selected, resolved ^1H NMR resonances versus total Ca^{2+} concentration for 5.5 mM E60Q (initial concentration). The intensities have been corrected for dilutions resulting from Ca^{2+} additions. (●) Ser24 NH; (○) Ser62 NH; (◇) resonance at 9.37 in one of the Ca_1 forms. (—) Best fit to the Ser24 NH data points, obtained with $\eta = 1.6$; (– –) calculated curve with $\eta = 1.0$; (···) calculated curve with $\eta = 2.6$; (–·–) curve calculated for a signal representing the Ca_2 form only. (B) Calculated intensities versus total Ca^{2+} concentration for signals from eq 1 with the following j's = 1: (1) j_0, j_B; (2) j_0, j_A; (3) j_0; (4) j_A, j_B, j_2; (5) j_B, j_2; (6) j_A, j_2; (7) j_2; (8) j_B; (9) j_A. All curves were calculated for 5.5 mM protein with $K_1 = K_2 = 8 \times 10^7$ M^{-1} and $\eta = K_B/K_A = 2.0$.

of the protein and the j's are either 1 or 0 depending on what species contribute to the intensity:

$$P_0 = 1/(1 + K_1Y + K_2Y^2)$$

$$P_A = K_AYP_0 \qquad P_B = K_BYP_0 \qquad P_2 = K_1K_2Y^2P_0$$

$$K_A = K_1/(1 + \eta) \qquad K_B = K_1 - K_A$$

where Y is the concentration of free Ca^{2+} ion given by

$$Y = \mathrm{CATOT}_i - \frac{F\mathrm{CP}_i(K_1Y + 2K_1K_2Y^2)}{1 + K_1Y + K_1K_2Y^2}$$

where CATOT_i and CP_i have been corrected for dilution and K_1 and K_2 have the values as determined from the titrations in the presence of chelator. Y has to be solved iteratively for each titration point, i. The variable parameters η, F, and IMAX are varied to minimize the error square sum given by

$$\mathrm{ESS} = \sum_i (I_{\mathrm{calculated},i} - I_{\mathrm{measured},i})^2$$

The error limits for η were obtained by fixing η, minimizing ESS for this value of η by adjusting the other variable parameters, fixing η at a new value, minimizing ESS, etc. The ESS was then plotted versus η, as exemplified in Figure 4, and the error limits were taken to include all limits of η giving less than two times the ESS of the optimal fit.

K^+ Binding. Two-dimensional ^1H NMR (COSY) spectra were recorded for 5 mM Ca^{2+}-free calbindin (wild type) in H_2O (5% D_2O) at pH 7.5 and 27 °C in the absence and

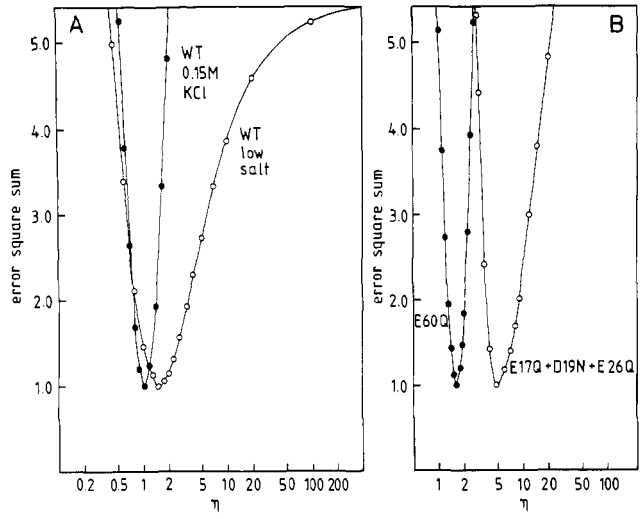

FIGURE 4: Error square sum (ESS) versus log η. These curves were obtained by fixing η at different values and adjusting the other variable parameters (IMAX and F) to obtain the best possible fit for each value of η. (A) (○) Wild type at conditions resembling 0.05 M KCl; (●) wild type at 0.15 M KCl. (B) (●) E60Q and (○) (E17Q+D19N+E26Q) at conditions resembling 0.05 M KCl.

presence of 0.15 M KCl. ^{39}K NMR spectra were obtained at 16.88 MHz on a Nicolet 360 WB spectrometer using a homemade horizontal probe with a solenoidal coil as described (Neurohr et al., 1983). The Ca^{2+}-free wild-type calbindin was titrated with KCl, at increasing intervals between 1 mM and 1 M KCl. The maximum K^+ affinity for the proteins was determined from least-squares fits to the line width of the ^{39}K NMR resonance as a function of total K^+ concentration (Forsén et al., 1987).

^{113}Cd NMR. ^{113}Cd NMR spectra were obtained at 56.55 MHz on a homemade spectrometer (Drakenberg et al., 1983). The normal one-pulse experiment was used and 25 000–100 000 transients were accumulated, with a pulse length of 10 μs (45°) and a pulse repetition time of 0.5 s. Spectra were recorded for 2–3 mM protein at pH 6.5 and 25 °C, and $^{113}Cd(NO_3)_2$ was added stepwise with 0.15–0.20 mol of Cd^{2+}/mol of protein in each addition. Spectral shifts are reported relative to 0.1 M $^{113}Cd(ClO_4)_2$ at pH 7.0.

Results and Discussion

The aim of this work has been to study the salt dependence of the Ca^{2+} affinity and cooperativity of bovine calbindin D_{9k} and a series of mutants with reduced surface charge. The macroscopic Ca^{2+}-binding constants, K_1 and K_2 (Table II), were obtained from titrations in the presence of a Ca^{2+} chelator as exemplified in Figure 5. K_1 and K_2, expressed in molar concentration units, were used to calculate the free energy of binding of two Ca^{2+} ions, $\Delta G_{tot} = -RT \ln (K_1K_2)$, and a lower limit of the free energy of interaction between the sites (cf. below), $-\Delta\Delta G_{\eta=1} = RT \ln (4K_2/K_1)$, as displayed in panels A and B of Figure 6, respectively. The salt effects on calcium affinity are similar to those obtained for small, highly negatively charged chelating agents like EDTA and EGTA analogues (Harafuji & Ogawa, 1980; Sillén & Martell, 1964; e.g., the chelators used in this study, cf. Experimental Procedures). Addition of 0.15 M KCl changes the free energy of binding of two Ca^{2+} ions to the wild-type protein by 23 kJ·mol^{-1}, corresponding to a 10^4-fold decrease in the product of K_1 and K_2.

K^+ Binding. Part of the decrease in Ca^{2+} affinity upon addition of KCl could reflect competition between K^+ and Ca^{2+} for the Ca^{2+} sites rather than pure ionic strength effects

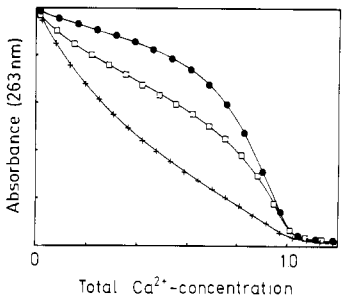

FIGURE 5: Examples of experimental data (absorbance at 263 nm versus total Ca^{2+} concentration) from Ca^{2+} titrations of 5,5'-Br_2BAPTA in the presence of mutant calbindins D_{9k} at low salt concentration together with curves of optimal fit to the data points (log K_1, log K_2 in square brackets): (●) E17Q [7.3, 8.2], (□) (E17Q+E26Q) [6.8, 7.8], (+) (E17Q+D19N+E26Q) [6.8, 6.7]. In the figure $[Ca^{2+}]_{tot}$ is normalized such that $[5,5'\text{-}Br_2BAPTA]_{tot} + 2[calbindin]_{tot} = 1.0$.

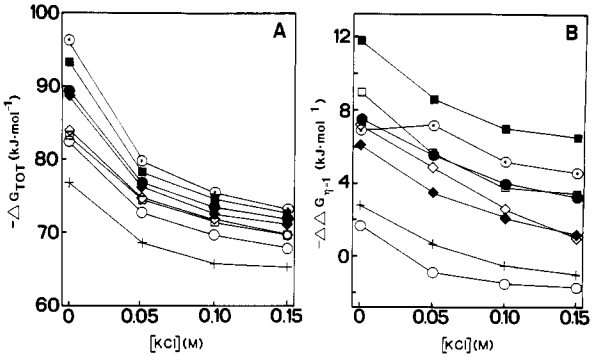

FIGURE 6: (A) Free energy of binding of two Ca^{2+} ions, ΔG_{tot}, and (B) the lower limit of the free energy of interaction between the two Ca^{2+} sites, $-\Delta\Delta G_{\eta=1}$, as a function of KCl concentration for (⊙) the wild-type protein, (●) E17Q, (◆) D19N, (■) E26Q, (○) (E17Q+D19N), (□) (E17Q+E26Q), (◇) (D19N+E26Q), and (+) (E17Q+D19N+E26Q). The uncertainties in ΔG_{tot} are less than ±0.5 kJ·mol^{-1} and in $-\Delta\Delta G_{\eta=1}$ are generally ±1 kJ·mol^{-1}. For clarity E60Q is not included in the figures. ΔG_{tot} of E60Q falls in between the numbers for the wildtype and E26Q, and $-\Delta\Delta G_{\eta=1}$ lies close to the value of D19N at all values of KCl concentration studied.

(screening of electrostatic interactions and change in activity coefficients). To investigate this point, 2D ^{1}H NMR COSY spectra were recorded for Ca^{2+}-free calbindin (wild type) at pH 7.5 and 27 °C in the absence and presence of 0.15 M KCl. Sixty-seven backbone NH–C_αH cross-peaks were found in both cases (4 missing, most likely due to fast exchange), and the average shift difference was 0.02 ppm for NH and 0.01 ppm for C_αH, the largest change being 0.07 ppm. In contrast, Ca^{2+} addition causes shift changes as large as 2.4 ppm for NH and 0.6 ppm for C_αH (Skelton et al., 1990a,b). This indicates that the binding of K^+ ions has only a minimal effect on the calbindin structure. In addition, the titration of Ca^{2+}-free wild-type calbindin with KCl, monitored by ^{39}K NMR, indicated a maximal affinity of log K = 2.5 for binding of one or two K^+ ions plus weak association of additional K^+ ions (log $K \simeq 1$). Thus, the larger and monovalent K^+ ions seem to associate at the negatively charged surface of calbindin but do not bind in the same way as do Ca^{2+} ions. It is likely that in the absence of Ca^{2+} the Ca^{2+} ligands repel each other and cannot fold in the proper conformation for Ca^{2+} coordination. It has been suggested that the charge on K^+ is too low to overcome the ligand repulsion and that K^+ binding would not result in the same arrangement of the ligands as in the Ca^{2+}-bound state (Snyder et al., 1990).

Structural Effects of Mutations: ^{1}*H NMR*. When interpreting the results for mutant proteins, it is important to know

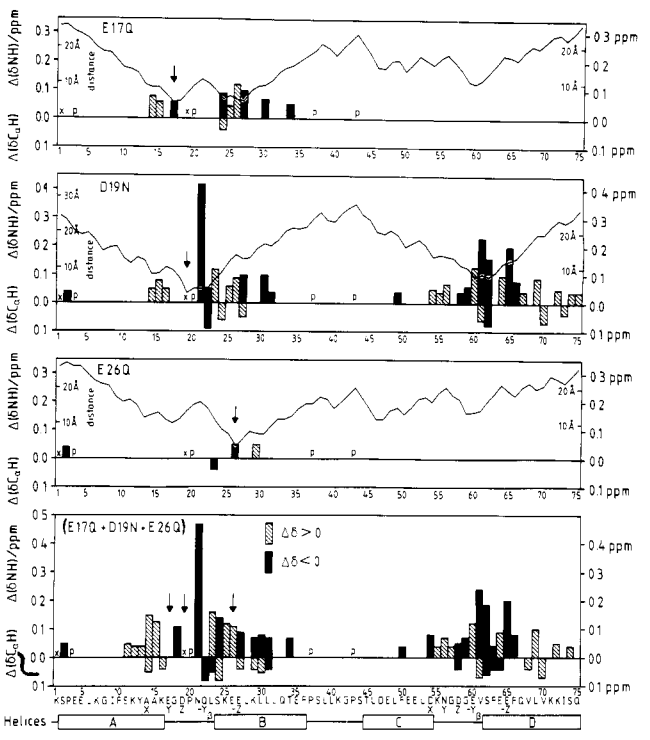

FIGURE 7: Chemical shift differences $\Delta(\delta)$ between mutant and wild-type protein. For each mutant $\Delta(\delta$NH) for each residue is represented by a vertical bar above the 0 line and $\Delta(\delta C_\alpha H)$ is shown below the line. Black bars are used when the chemical shift is larger in the wild type than in the mutant (mutation results in an upfield shift), and shaded bars are used when the chemical shift is smaller in the wild type (mutation results in a downfield shift). E17Q (top), D19N (second from top), E26Q (third from top), and (E17Q+D19N+E26Q) (bottom). x = not assigned; P = proline. Effects ≤0.03 ppm are not displayed. For a single mutants the shortest of the distances from the NH or C_αH to the midpoint between the oxygens in the substituted carboxylate group (in the crystal structure) is drawn as a curve connecting the values for each residue. Arrows indicate the site of mutation. The sequence is given as in the wild-type protein.

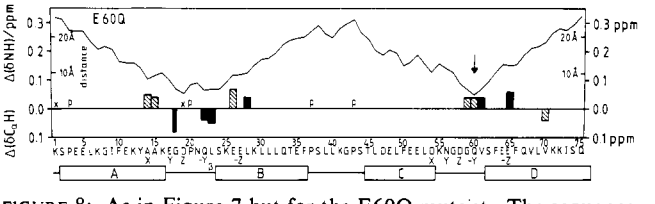

FIGURE 8: As in Figure 7 but for the E60Q mutant. The sequence is given for this mutant.

whether the structural changes caused by the mutation are large or small and if they are confined to the site of mutation or propagate into other regions. One approach to this problem is to record 2D ^{1}H NMR spectra, assign the backbone resonances, and compare chemical shifts, NOE patterns, and ^3J coupling constants with the wild-type protein. In the present work the backbone NH and C_αH resonances have been assigned for the Ca-loaded forms of the single mutants E17Q, D19N, E26Q, and E60Q, the double mutant (E17Q+E26Q), and the triple mutant (E17Q+D19N+E26Q). The comparison with the chemical shifts in the Ca-loaded wild-type protein is presented in Figures 7–9. It is striking how well the chemical shift effects in the double and triple mutants agree with the sum of the effects in the constituent single mutants. The very modest shift changes observed for E17Q, E26Q, (E17Q+E26Q), and E60Q indicate that the structures of these proteins are nearly identical with the wild-type structure. The very small shift effects observed close to the site of mutation are most likely direct effects of substituting an amide group

Table II: Macroscopic Calcium-Binding Constants, K_1 and K_2[a]

protein	0.00 M KCl		0.05 M KCl		0.10 M KCl		0.15 M KCl	
	log K_1	log K_2	log K_1	log K_2	log K_1	log K_2	log K_1	log K_2
wild type	8.2	8.6	6.7	7.2	6.5	6.8	6.3	6.5
E17Q	7.4 ± 0.3	8.1 ± 0.3	6.5 ± 0.3	7.0 ± 0.3	6.3 ± 0.2	6.5 ± 0.2	6.2 ± 0.2	6.4 ± 0.2
D19N	7.5	8.0	6.7	6.7	6.5	6.2	6.5	6.0
E26Q	7.6 ± 0.3	8.7 ± 0.3	6.5 ± 0.2	7.3 ± 0.2	6.2 ± 0.2	6.9 ± 0.2	6.1	6.6
(E17Q+D19N)	7.4	7.1	6.8	6.0	6.5	5.7	6.3	5.5
(E17Q+E26Q)	6.8 ± 0.3	7.8 ± 0.3	6.4	6.7	6.2	6.3	6.1	6.1
(D19N+E26Q)	7.1	7.8	6.4	6.7	6.2	6.3	6.1	6.1
(E17Q+D19N+E26Q)	6.8	6.7	6.3	5.8	6.1	5.4	6.1	5.3
E60Q	8.0	8.5	6.9	6.9	6.8	6.4	6.6	6.2

[a] K_1 and K_2 are in molar concentration units. The uncertainties are less than ±0.1 unless indicated. The values of K_1 and K_2 for the wild type are slightly different from the numbers previously reported (Linse et al., 1987, 1988) because the old results were obtained on a partly deamidated sample (Chazin et al., 1989). Other changes are due to the fact that we have now produced apoprotein samples with lower residual Ca^{2+}, and we have thus been able to obtain more data points in the very beginning of the titrations.

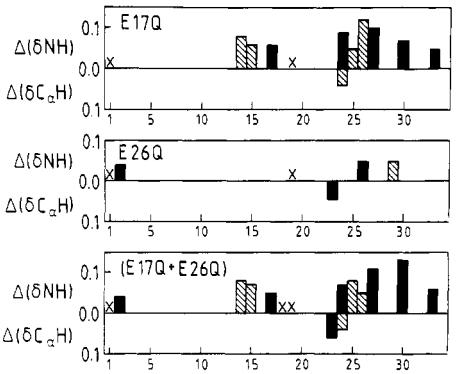

FIGURE 9: As in Figure 7 but displaying only the region where shift changes do occur for E17Q (top), E26Q (middle), and (E17Q+E26Q) (bottom). No distances are drawn in this plot.

for a carboxyl group. Somewhat larger effects are observed in the Ca^{2+}-binding region of D19N and the triple mutant, although these effects are far smaller than the effects of removing Ca^{2+} from the wild type (Skelton et al., 1990a,b; cf. above). There also appears to be an inverse relationship between the change in chemical shift of a proton and its proximity to the Asp19 side chain in the wild-type crystal structure. The largest shift effect (0.45 ppm upfield) is observed for the N21 NH. In the crystal the Asp19 carboxylate group appears hydrogen bonded to the Asn21 NH, and there is also indication of a weak hydrogen bond from the Asn21 NH to the Asp19 carbonyl oxygen. A molecular dynamics simulation of calbindin D_{9k} (Ahlström et al., 1989) indicates that the Asn21 NH participates in a rather flexible hydrogen bond mostly involving the Asp19 carboxylate, but also the Asp19 carbonyl [cf. Linse et al. (1990)]. In both cases the Asn21 NH is located in close proximity to the Asp19 side chain, and the substitution of an amide for the Asp19 carboxylate could thus be expected to cause large shift perturbations even if no structural changes occur. Thus it is not possible to judge solely from the observed shift effect if any localized rearrangement occurs around Asp19 and Asn21.

Therefore, the pattern of NOE's (NH–NH, N–C_αH, C_αH–C_αH) was investigated for the triple mutant and compared to the wild type (Kördel et al., 1989, Figures 4–6). The only significant difference in sequential NH–NH connectivities is that the triple mutant lacks the E60–V61 connectivity reported as weak in the wild type. Only minor differences were observed in the NOE connectivities within the short antiparallel β-sheet between the two loops as displayed in Figure 10. It is clear that the β-sheet is present also in the mutant, but the N21 C_αH to Q22 NH connectivity is missing in the mutant. Thus there appears to be some rearrangement at the Asn21 end of the β-sheet, which might imply a slight weakening of the β-sheet

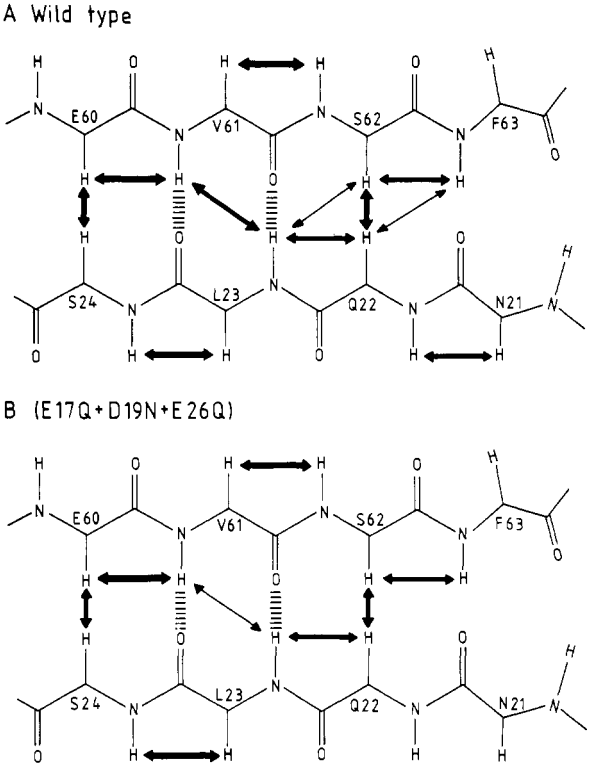

FIGURE 10: The short antiparallel β-sheet. Observed NOE connectivities (in 200-ms NOESY spectra) are indicated with double-headed arrows giving a qualitative measure of the relative strength of the NOE's. Crosshatched vertical bars show the hydrogen bonds that can be deduced from the displayed connectivities. (A) Wild-type protein as previously presented (Kördel et al., 1989) and redrawn from Figure 6 in that reference; (B) (E17Q+D19N+E26Q).

interaction between the two sites. This could be propagated effects of perturbations of the interaction between the Asn21 NH and Asp19 side chain when the latter is replaced by an amide.

Structural Effects of Mutations: ^{113}Cd *NMR*. The ^{113}Cd NMR shifts of both metal ion sites have been measured during Cd titrations of the wild-type and mutant calbindins as summarized in Table III. Cd^{2+} binds in a sequential manner to all these proteins and site II is filled first. A sharp resonance of Cd^{2+} in site II is seen when less than 1.0 equiv of Cd^{2+} is added. At a higher cadmium concentration this resonance is slightly broadened and displaced toward lower frequency, maximum displacement 5 ppm, as a result of Cd^{2+} entering site I. In addition, a new broad resonance of Cd^{2+} in site I appears at lower frequency. Site I in calbindin is not a standard EF-hand site, but contains two additional amino acids in the loop (the "pseudo EF hand"), and the ^{113}Cd shift is

Table III: ^{113}Cd NMR Chemical Shifts (in ppm) for Cd^{2+} Ions Bound to Calbindin Wild Type and Mutants and ^{113}Cd Shift Displacement, $\Delta\delta_{II,I}$, of the Site II Shift on Cd^{2+} Binding to Site I[a]

protein	≤1 equiv of Cd, site II	2 equiv of Cd		$\Delta\delta_{II,I}$
		site II	site I	
wild type[b]	−105	−110	−156	5
E17Q	−105.8	−109.3	−148	3.5
D19N	−106.5	−108.6	−135	2.1
E26Q	−104.8	−109.6	−150	4.8
(E17Q+D19N)	−106.8	−107.2	−138	0.4
(E17Q+E26Q)	−106	−108	−145	2
(D19N+E26Q)	−105.8	−107.5	−138	1.7
(E17Q+D19N+E26Q)	−106.5	−106.5	−135	0.0
E60Q	−106.9	−111.8	nd[c]	4.9

[a] The estimated maximum error in the chemical shift is 0.5 ppm for ^{113}Cd bound to site II and 10 ppm for ^{113}Cd bound to site I. The maximum error in $\Delta\delta_{II,I}$ is thus 1.0 ppm. [b] Values from Linse et al. (1987). [c] nd = not determined.

slightly lower than observed for normal EF hands (cf. below). ^{113}Cd NMR shifts are extremely sensitive to the charge distribution around the Cd^{2+} ion, and the reported shifts for Cd^{2+} ions bound to various proteins range from −193 to 751 ppm, with those of EF hands (calmodulin, parvalbumin, troponin C, and calbindin) lying between −130 and −88 ppm [cf. Table 2 in Johansson and Drakenberg (1990)]. The effects on the ^{113}Cd resonance of site II on mutation are thus extremely small and indicate that the fold of this site is nearly identical in the wild-type and all mutant proteins. There are nevertheless significant differences in $\Delta\delta_{II,I}$, the shift displacement of the site II resonance on Cd^{2+} binding to site I. A value of $\Delta\delta_{II,I} \neq 0$ indicates that the sites do interact; i.e., Cd^{2+} binding to site I affects site II. For the wild type, E26Q, and E60Q the $\Delta\delta_{II,I}$ is around 5 ppm, but for (E17Q+D19N) and (E17Q+D19N+E26Q) $\Delta\delta_{II,I}$ is close to 0 ppm (cf. Table III); this indicates that there are differences in the extent of site–site interaction between the different proteins. The somewhat larger variations in the frequency of the broad resonance from cadmium in site I are also small considering the large shift range for ^{113}Cd. For mutants in which Asp19 is not altered, it is reasonable to conclude that the conformation of site I is largely unperturbed by the surface charge annihilations, whereas the D19N mutation appears to cause some small-scale rearrangement of this site.

Salt Effects on Mutant Proteins. The differences in Ca^{2+} affinity among the individual proteins are, as expected, most pronounced at low ionic strength, and the salt effect on ΔG_{tot} becomes smaller as more charges are eliminated. For single mutants ΔG_{tot} changes by 17 (E17Q and D19N) or 21 kJ·mol^{-1} (E26Q and E60Q) on addition of 0.15 M KCl. For mutants with two charges neutralized the change is 14–15 kJ·mol^{-1} and for the triple mutant 12 kJ·mol^{-1}. The difference in ΔG_{tot} between the triple mutant and wild type is thus 19 kJ·mol^{-1} at low ionic strength (no added KCl) and 8 kJ·mol^{-1} at 0.15 M KCl. This means that neutralization of three charges leads to a 2000-fold reduction in K_1K_2 at low ionic strength and to a 25-fold reduction at 0.15 M KCl. The finding that protein surface charges may influence the strength of ion binding significantly (Linse et al., 1988) thus pertains also to physiological ionic strength.

If we compare the effects of individual mutations, it is clear that the contributions to ΔG_{tot} from the negative side chains of Glu17, Asp19, Glu26, and Glu60 are not equal. Glu26 is situated further away from the Ca^{2+} ions (cf. Figure 1) and contributes only half as much to the free energy of binding as does either Glu17 or Asp19. In the crystal structure (Szebenyi & Moffat, 1986) the side chain of Glu60 is located between the two Ca^{2+} ions (cf. Figure 1) and faces the surrounding water. Surprisingly, however, the substitution of Gln for Glu60 has only a minor effect on ΔG_{tot}. Also, the salt effect on the interaction between the carboxylate group of Glu60 and the Ca^{2+} ions, which is given by the difference in the salt effects on ΔG_{tot} of the wild type and E60Q mutant, is only 2 kJ·mol^{-1} (comparing low salt concentration and 0.15 M KCl). In contrast, the salt effects on the interactions between the Ca^{2+} ions and the Glu17 and Asp19 carboxylates, which are close to both Ca^{2+} sites, but in fact not as close as Glu60 (cf. Figure 1), are as large as 6 kJ·mol^{-1} for each carboxylate. The Glu60 side chain thus does not appear to function as a surface charge. One possible explanation for the observed results is that in solution Glu60 actually ligates the Ca^{2+} ion in site I, as was found in a molecular dynamics simulation of calbindin D_{9k} (Ahlström et al., 1989). In support of this interpretation is the finding that the binding free energy is very similar when the ligating carbonyl oxygen is provided by a carboxylate or amide group; the effect on ΔG_{tot} by the E60Q mutation (+1.8 ± 1.0 kJ·mol^{-1}) is similar in magnitude to that of N56D (−1.1 ± 1.0 kJ·mol^{-1}; S. Linse, unpublished result), in which the ligating amide group of N56 is replaced by a carboxylate group. Further support comes from studies of the mutant E60D, for which the calcium affinity is significantly reduced as compared to the wild type (+7.0 ± 1.0 kJ·mol^{-1}; Brodin and Linse, unpublished result). The side chain of Asp60 in this mutant protein is maybe too short to reach over to ligate the Ca^{2+} ion in site I.

Cooperativity. The cooperativity can be characterized by $\Delta\Delta G$, the effect of Ca^{2+} binding to one of the sites on the free energy of Ca^{2+} binding to the other site.

$$\Delta\Delta G = \Delta G_{I,II} - \Delta G_I = \Delta G_{II,I} - \Delta G_{II} = -RT \ln (K_{I,II}/K_I) = -RT \ln (K_{II,I}/K_{II})$$

where the ΔG variables are defined in Figure 2 and the K terms are the corresponding microscopic (site) binding constants. The titrations in the presence of Quin 2 (or 5,5′-Br_2BAPTA) do not sense the distribution of Ca^{2+} between the two sites of the protein and hence yield only the macroscopic binding constants, which refer to the binding of the first and second Ca^{2+} ion irrespective of which site is occupied in the protein.

Table IV: Relative Affinity for Two Sites, η, and Free Energy of Interaction between the Sites, $\Delta\Delta G$, for Wild-Type and Selected Mutant Calbindins[a]

protein	[KCl] (M)	η of best fit	η range	$-\Delta\Delta G_{\eta=1}$	$RT \ln [(\eta+1)^2/4\eta]$	$-\Delta\Delta G$
wild type	0.15	1.0	1.0–1.5	4.6 ± 0.8	0.05 ± 0.05	4.6 ± 0.9
wild type	0.05	1.6	1.0–3.0	7.2 ± 1.0	0.4 ± 0.4	7.7 ± 1.7
D19N	0.05	1.4	1.0–4.0	3.5 ± 1.0	0.5 ± 0.5	4.0 ± 1.5
(E17Q+D19N)	0.05	4.9	3.5–7.0	−0.9 ± 1.3	1.6 ± 0.4	0.7 ± 1.7
(E17Q+D19N+E26Q)	0.05	4.8	3.7–6.5	0.7 ± 0.4	1.4 ± 0.4	2.1 ± 0.8
E60Q	0.05	1.6	1.3–2.0	3.3 ± 0.8	0.1 ± 0.1	3.4 ± 0.9

[a] η is defined here as K_B/K_A, where B refers to the site with the higher affinity. All values for η are thus ≥1, and it has not been determined which site in the protein is the stronger. Since the error limits of η are not symmetrical around the value of η obtained from the best fit to the experimental data, the estimated maximum errors are given as a range for η.

We therefore use the relations between macroscopic and microscopic binding constants

$$K_1 = K_I + K_{II}$$

$$K_1K_2 = K_IK_{II,I} = K_{II}K_{I,II}$$

and write

$$-\Delta\Delta G = RT \ln (4K_2/K_1) + RT \ln [(\eta + 1)^2/4\eta]$$

where $\eta = K_{II}/K_I$. The second term has a minimum (of zero) for $\eta = 1$, and we may thus obtain a lower limit of $-\Delta\Delta G$ solely from the macroscopic binding constants as

$$-\Delta\Delta G_{\eta=1} = RT \ln (4K_2/K_1)$$

As can be seen in Figure 5B, $-\Delta\Delta G_{\eta=1}$ decreases with increasing salt concentration, and there are differences among the various proteins. The effects of the individual substitutions on $-\Delta\Delta G_{\eta=1}$ appear to be at least qualitatively additive. For instance, the slight increase in $-\Delta\Delta G_{\eta=1}$ observed for the E26Q mutant, as compared to the wild type, is paralleled with a similar increase for (E17Q+D19N+E26Q) as compared to (E17Q+D19N). However, since mutations could alter either $\Delta\Delta G$ or η or both, the salt effects on $\Delta\Delta G$ do not follow directly from the results in Figure 5B. If we combine the results from the titrations in the presence of chelator with the information on η that can be derived from Ca^{2+} titrations monitored by ^1H NMR, it is possible to assess the effects on $\Delta\Delta G$ of charge neutralization and added electrolyte (Table IV). We can thus conclude that the positive cooperativity ($\Delta\Delta G < 0$) of Ca^{2+} binding observed under low ionic strength conditions (Linse et al., 1987) is not eliminated at physiological salt concentration in the wild type nor in most surface charge mutants. A value of $-\Delta\Delta G_{\eta=1} = 5$ kJ·mol^{-1} (wild type at 0.10–0.15 M KCl) corresponds to an at least 8-fold increase in the Ca^{2+} affinity for site I as a result of Ca^{2+} binding at site II (and vice versa); i.e., $K_{I,II}/K_I = K_{II,I}/K_{II} \geq 8$. We can also conclude that the cooperativity is significantly lower in (E17Q+D19N) and (E17Q+D19N+E26Q) than in the wild-type calbindin and that the substitutions D19N and E60Q decrease the cooperativity. There appears to be some correlation between the cooperativity and the ^{113}Cd shift displacement, $\Delta\delta_{II,I}$ (Table III). In this context it is also interesting to ask whether the low cooperativity in the triple mutant is to any extent caused by the small reorganization at the N21 end of the β-sheet between the Ca^{2+} loops as inferred from the NOE data (cf. above and Figure 10). By investigating the structural organization of protein polar groups in calbindin D_{9k}, Wesolowski et al. (1990) have suggested specific structures of mutually coupled groups that transmit local structural and charge density perturbations induced by an ion over long distances. These structures involve two chains through the β-sheet that transmit effects of Ca^{2+} binding at one site to the other site (Wesolowski et al., 1990). Whether the observed effects on the cooperativity in E60Q, (E17Q+D19N), and (E17Q+D19N+E26Q) result from perturbation of any of the suggested chains (starting at Gln22 C=O and Glu60 C=O, respectively) remains to be investigated in a more detailed structural analysis of these mutants involving complete assignments, extensive NOE data, NH exchange rates in the absence and presence of Ca^{2+}, etc.

The present experimental study of wild-type and mutant bovine calbindins D_{9k}, encompassing both the contribution of individual charges to the free energy of binding of two Ca^{2+} ions and the salt dependence of this thermodynamic parameter, may serve as a starting point for evaluation of different models for electrostatic interactions in proteins.

ACKNOWLEDGMENTS

We thank Eva Thulin and Ingrid Andersson for the purifications and preparations of Ca^{2+}-free proteins and Mats Lundell for help with the illustrations. We gratefully acknowledge Jannette Carey for helpful comments on the manuscript.

Registry No. L-Glu, 56-86-0; L-Asp, 56-84-8; Ca, 7440-70-2; Cd, 7440-43-9.

REFERENCES

Ahlström, P., Teleman, O., Kördel, J., Forsén, S., & Jönsson, B. (1989) *Biochemistry 28*, 3205–3211.

Akke, M., & Forsén, S. (1990) *Proteins: Struct., Funct., Genet. 8*, 23–29.

Bredderman, P. J., & Wasserman, R. H. (1974) *Biochemistry 13*, 1687–1694.

Brodin, P., Grundström, T., Hofmann, T., Drakenberg, T., Thulin, E., & Forsén, S. (1986) *Biochemistry 25*, 5371–5377.

Bryant, D. T. W. (1985) *Biochem. J. 226*, 613–616.

Bryant, D. T. W., & Andrews, P. (1984) *Biochem. J. 219*, 287–292.

Chazin, W. J., Kördel, J., Thulin, E., Hofmann, T., Drakenberg, T., & Forsén, S. (1989) *Biochemistry 28*, 8646–8653.

Drakenberg, T., Forsén, S., & Lilja, H. (1983) *J. Magn. Reson. 53*, 412–422.

Drakenberg, T., Hofmann, T., & Chazin, W. J. (1989) *Biochemistry 28*, 5946–5954.

Forsén, S., Drakenberg, T., & Wennerström, H. (1987) *Q. Rev. Biophys. 19*, 83–114.

Gilson, M. K., & Honig, B. H. (1987) *Nature 330*, 84–86.

Harafuji, H., & Ogawa, Y. (1980) *J. Biochem. 87*, 1305–1312.

Harvey, S. C. (1989) *Proteins: Struct., Funct., Genet. 5*, 78–92.

Honig, B., & Gilson, M. K. (1988) *Proteins: Struct., Funct., Genet. 3*, 32–52.

Johansson, C., & Drakenberg, T. (1990) in *Annual Reports on NMR Spectroscopy* (Webb, G. A., Ed.) pp 1–59, Academic Press, London.

Johansson, C., Brodin, P., Grundström, T., Thulin, E., Forsén, S., & Drakenberg, T. (1990) *Eur. J. Biochem. 187*, 455–460.

Kördel, J., Forsén, S., & Chazin, W. J. (1989) *Biochemistry 28*, 7065–7074.

Kretsinger, R. H. (1987) in *Cold Spring Harbor Symposia on Quantitative Biology*, Vol. LII, pp 499–510, Cold Spring Harbor Laboratory, Cold Spring Harbor, NY.

Kretsinger, R. H., & Nockolds, C. E. J. (1973) *J. Biol. Chem. 248*, 3313–3326.

Linse, S., Brodin, P., Drakenberg, T., Thulin, E., Sellers, P., Elmdén, K., Grundström, T., & Forsén, S. (1987) *Biochemistry 26*, 6723–6735.

Linse, S., Brodin, P., Johansson, C., Thulin, E., Grundström, T., & Forsén, S. (1988) *Nature 335*, 651–652.

Linse, S., Teleman, O., & Drakenberg, T. (1990) *Biochemistry 29*, 5925–5934.

Long, J. E., Durham, B., Okamura, M., & Millett, F. (1989) *Biochemistry 28*, 6970–6974.

MacKinnon, R., Latorre, R., & Miller, C. (1989) *Biochemistry 28*, 8092–8099.

Martin, S. R., Linse, S., Johansson, C., Bayley, P. M., & Forsén, S. (1990) *Biochemistry 29*, 4188–4193.

Neurohr, K. J., Drakenberg, T., Forsén, S., & Lilja, H. (1983) *J. Magn. Reson. 51*, 460–469.

Sillén, L. G., & Martell, A. E. (1964) *Stability Constants of Metal-Ion Complexes*, The Chemical Society, London.
Skelton, N. J., Kördel, J., Forsén, S., & Chazin, W. J. (1990a) *J. Mol. Biol. 213*, 593-598.
Skelton, N. J., Forsén, S., & Chazin, W. J. (1990b) *Biochemistry 29*, 5752-5761.
Snyder, E. E., Buoscio, B. W., & Falke, J. J. (1990) *Biochemistry 29*, 3937-3943.
Sternberg, J. E., Hayes, F. R. F., Rusell, A. J., Thomas, P. G., & Fersht, A. R. (1987) *Nature 330*, 86-88.
Svensson, B., Jönsson, B., & Woodward, C. (1990a) *Biophys. Chem.* (in press).
Svensson, B., Jönsson, B., & Woodward, C. (1990b) *Biochemistry* (submitted for publication).
Szebenyi, D. M. E., & Moffat, K. (1986) *J. Biol. Chem. 261*, 8761-8777.
Thomas, P. G., Russell, A. J., & Fersht, A. R. (1985) *Nature 318*, 375-376.
Tsien, R. (1980) *Biochemistry 19*, 2396-2404.
Weber, G. (1975) *Adv. Protein Chem. 29*, 1-83.
Weber, P. C., Lukas, T. J., Craig, T. A., Wilson, E., King, M. M., Kwiatkowski, A. P., & Wattersson, D. M. (1989) *Proteins: Struct., Funct., Genet. 6*, 70-85.
Wendt, B., Hofmann, T., Martin, S., Bayley, P., Brodin, P., Grundström, T., Thulin, E., Linse, S., & Forsén, S. (1988) *Eur. J. Biochem. 175*, 435-445.
Wesolowski, T. A., Boguta, G., & Bierzynski, A. (1990) *Protein Eng.* (in press).

Polymerization Site in the β Chain of Fibrin: Mapping of the Bβ1-55 Sequence†

Bharat V. Pandya,‡ Jerome L. Gabriel,§ Joseph O'Brien,§ and Andrei Z. Budzynski*,§
Department of Biochemistry, Kirksville College of Osteopathic Medicine, Kirksville, Missouri 63501, and Department of Biochemistry, Temple University School of Medicine, Philadelphia, Pennsylvania 19140
Received August 7, 1990

ABSTRACT: The formation of a fibrin clot occurs through binding of putative complementary sites, called fibrin polymerization sites, located in the NH_2- and COOH-terminal domains of fibrin monomer molecules. In this study, we have investigated the structure of the NH_2-terminal fibrin polymerization site by using fibrinogen-derived peptides and fragments. Fibrinogen was digested with *Crotalus atrox* protease III, to two major molecular species: a M_r 325 000 derivative (Fg325) and a peptide of M_r 5000. The peptide and its thrombin-cleavage product were purified by ion-exchange and reverse-phase HPLC; the authenticity of the Bβ1-42 and β15-42 peptides, respectively, was confirmed by amino acid sequencing. Since Fg325 had decreased thrombin coagulability, we addressed the question of whether the peptide Bβ1-42 contained a fibrin polymerization site. In other to identify and map the site, the peptides Bβ1-42 and β15-42 were tested for their ability to inhibit fibrin monomer polymerization. In addition the following peptides prepared by chemical synthesis were also tested: β15-18, β15-26, β24-42, β40-54, β50-55, and α17-19-Pro. While Bβ1-42 had no inhibitory activity, the peptide devoid of fibrinopeptide B, β15-42, was a strong inhibitor. The peptides β15-18, β15-26, and β15-42 decreased the rate of fibrin polymerization by 50% at a molar excess of the peptide to fibrin monomer of 500, 430, and 50, respectively. The peptides β24-42, β40-54, and β50-55 were inactive. Computer-aided prediction of probable secondary structures in Bβ1-55, together with polymerization inhibition by β15-55-derived peptides, suggested that the polymerization site in the amino-terminal domain of the β chain might be composed of noncontiguous amino acids. However, the NH_2-terminal disulfide knot of fibrin, which contains amino termini of the α, β, and γ chains, not only was a stronger inhibitor of polymerization than β15-42, but it also had a higher affinity for binding to fibrin monomer. Therefore, it is proposed that the fibrin polymerization site in the NH_2-terminal domain of fibrin may be composed of sequence derived from both the α and β chains.

Human fibrinogen is a large and complex plasma glycoprotein made up of pairs of three nonidentical polypeptide chains: Aα, Bβ, and γ (Doolittle, 1984; Budzynski, 1986). Conversion of fibrinogen to fibrin, which involves cleavage of fibrinopeptide A and fibrinopeptide B from the NH_2 termini of the Aα and Bβ chains of fibrinogen, respectively, is essential for blood clot generation. The formation of an insoluble fibrin clot can be divided into three steps: (a) the removal of fibrinopeptides A and B to form fibrin monomer, (b) the self-polymerization of fibrin monomers to form a soluble clot, and (c) the formation of covalent cross-links by factor XIIIa to form a stable clot. The exact sites of the actions of thrombin and factor XIIIa are known. However, the mechanism of polymerization and amino acid residues of the fibrinogen molecule involved in the polymerization reaction remain to be described. Binding phenomena of fibrinogen, fibrin monomer, and their degradation products have enabled development of a model for the mechanism of fibrin polymerization (Kudryk et al., 1974; Blombäck et al., 1978; Olexa & Budzynski, 1979, 1980). An essential concept of this model is that the thrombin-induced cleavage of the Aα and Bβ chains in the NH_2-terminal domain exposes binding sites, called fibrin polymerization sites, that are complementary to the binding sites preexistent in the COOH-terminal domain of the fibrinogen molecule (Budzynski et al., 1983). A polymerization site localized at the COOH-terminal domain of fibrinogen was postulated to be present within the sequence γ303-411 (Southan et al., 1985; Varadi & Scheraga, 1986). The preservation of the native conformation is essential for expression of polymerization sites in both the NH_2 (Budzynski et al., 1983) and the COOH terminus (Cierniewski et al.,

† This work was supported by Grant HL36221 from the National Heart, Lung and Blood Institute, National Institutes of Health, Bethesda, MD.
‡ Kirksville College.
§ Temple University.

0006-2960/91/0430-162$02.50/0